Journal of Cleaner Production 381 (2022) 135157

Contents lists available at ScienceDirect

Journal of Cleaner Production

journal homepage: www.elsevier.com/locate/jclepro

Influence of different chaotropic salts on etched mesoporous silica nanoparticles for the removal of bacteria DNA conveying antibiotic resistance genes from hospital wastewater

Adaora S. Ezeuko [a,c,*], Mike O. Ojemaye [a,c], Omobola O. Okoh [a,c], Anthony I. Okoh [b,c]

[a] Department of Pure and Applied Chemistry, University of Fort Hare, Alice, 5700, South Africa
[b] Department of Environmental Health Sciences, College of Health Sciences, University of Sharjah, Sharjah, United Arab Emirates
[c] SAMRC, Microbial Water Quality Monitoring Centre, University of Fort Hare, Alice, South Africa

ARTICLE INFO

Handling Editor: Maria Teresa Moreira

Keywords:
Mesoporous silica nanoparticles
Chaotropic salt
Enterococcus faecium
Adsorption
Heterogeneous
2M guanidine

ABSTRACT

The adsorption of bacteria DNA onto mesoporous silica nanoparticles in their original state has been a great challenge due to the high negative charge exhibited by both the DNA and silica surface. The aim of this study is to mediate bacteria DNA onto synthesized mesoporous silica nanoparticles (E-MSN) in combination with different chaotropic salts. E-MSN was synthesized via chemical etching techniques using sodium dodecyl sulfate (SDS) as an etchant. SDS was used to remove unwanted layers and provides a convenient platform for underlining mesopore with different chaotropic salts. Scanning electron microscopy (SEM) coupled with energy-dispersive x-ray spectroscopy (EDX), Fourier-transformed infrared spectroscopy (FTIR), x-ray diffraction spectroscopy (XRD), and point of zero charges (PZC) results showed that synthesized etched mesoporous silica nanoparticles have a crystalline, non-spherical shape and elemental composition of silica at approximately 2 Kev, functional groups that depict silica particles. Molecular characterization of extracted genes showed that *Enterococcus faecium* harbors *tetA*, *tetM*, and *ermB* in 201bp, 158bp, and 320bp, with the DNA purity ranging from 1.7 to 1.9. DNA adsorption was studied as a function of operating parameters in different solutions of chaotropic salts (sodium chloride (NaCl), 2 M guanidine HCl (CH_5N_3.HCl), and urea ($(NH_3)_2CO$). Among the different chaotropic salts used to compliment the silica nanoparticles, 2 M guanidine HCl exhibited the highest percentage (%) removal efficiency (90%) compared to urea (75%) and sodium chloride (70%) in simulated water and hospital wastewater. Experimental results revealed that the pseudo-second-order kinetic and Sips isotherm is the best fit for the adsorption process. Therefore, mesoporous silica nanoparticles enhanced by different chaotropic salts in this study showed that this material might be promising and economical for the uptake of bacteria DNA conveying antibiotics resistance genes from hospital wastewater.

1. Introduction

Recently, inorganic-based nanomaterials have gained much interest in wastewater treatment applications due to their inherent functionalities, such as size/shape-dependent morphology, scalability, easy synthesis, and stability (Kankala et al., 2020; Leonel et al., 2021; Maduraiveeran et al., 2019). These attractive features are responsible for their wide application in various fields such as engineering, agriculture, energy production, medicine, and wastewater treatment. Among numerous inorganic-based nanomaterials, mesoporous silica nanoparticles (MSN) have attracted the attention of researchers as promising adsorbents for the removal of different contaminants from water/wastewater. According to IUPAC, mesoporous is mesostructured material with a pore diameter between 2 nm and 50 nm and can be divided into silica-based material and non-silica-based material. The several mesostructured properties include narrow pore size distribution, controllable and uniform particle size, high specific surface area, large pore volume, ease of surface functionalization or surface modification, non-toxic nature, and colloidal stability, make it a suitable and efficient adsorbent for wastewater treatment process (Kankala et al., 2020; Panahi et al., 2019; Saman et al., 2020). MSN is thermally and chemically stable with controllable morphology and porosity in its original state (Kankala et al., 2020; Kumar et al., 2017). Both interior and exterior surfaces of MSN can undergo functionalization or modification

* Corresponding author. Department of Pure and Applied Chemistry, University of Fort Hare, Alice, 5700, South Africa.
E-mail addresses: adajesusd4@gmail.com, 201927090@ufh.ac.za (A.S. Ezeuko).

https://doi.org/10.1016/j.jclepro.2022.135157
Received 31 August 2022; Received in revised form 25 October 2022; Accepted 9 November 2022
Available online 15 November 2022

approaches by attaching multiple organic or inorganic functional groups via its Si–OH bond. Another intrinsic feature is that the silica interior surface can be a reservoir for loading guest molecules (Jafari et al., 2018). This feature could enhance the selective target of contaminants at the adsorptive site. Their pore size distribution (2 nm–30 nm) is usually narrow and can be controlled by changing the synthesis composition's mixture. The large surface area and pore size have been reported to have good sorption capability (Kumar et al., 2017), allowing well-controllable loading and release of DNA molecules (Li et al., 2012). Its adsorption mechanism is achieved mainly by electrostatic attraction and hydrogen bonding between positive contaminants and MSN.

Numerous synthesis route has been employed to achieve controllable morphological and porous structure/materials: they are (a) template-assisted techniques (Kumar et al., 2017), (b) sol-gel technique (Vazquez et al., 2017), (c) microwave-assisted techniques (de Greñu et al., 2020), and (d) chemical etching techniques (Salehtash et al., 2018). All these procedures successfully achieved a controllable morphology and particle size adequate for their diverse applications in science.

Studies have reported the effectiveness of MSN in the adsorption of cationic contaminants from water/wastewater (Abbaraju et al., 2009; Spoial et al., 2020). But few studies have reported the successful adsorption of anionic contaminants onto the negative surface of MSN. Numerous researchers have attempted to mediate duplex DNA onto MSN. These attempts were unsuccessful due to the repulsive effect between the bare MSN and DNA molecule (Jiang et al., 2021; Li et al., 2012). Besides, bacteria DNA is a bulky molecule with a high negative charge in its backbone. Therefore, in an aqueous solution, mediating it onto MSN mesopore with a negatively charged silica surface as an adsorbent is difficult. But reports have shown that adsorption of DNA onto MSN mesopore can be achieved when the silica surface undergoes modification or adding carriers (chaotropic salts) that would assist DNA adsorption onto MSN. For example, a study reported the successful adsorption of DNA onto MSN in the presence of multivalent cations (Solberg and Landry, 2006). Other studies functionalized the surface of MSN with a cationic linker (Gao et al., 2009) and the addition of 2 M Guanidine salt (chaotropic salt) at low pH in mediating DNA onto magnetic mesoporous silica nanoparticle (M-MSN).

Consequently, this study utilized, for the very first time, different chaotropic salts (sodium chloride, 2 M guanidine HCl and Urea) onto an etched mesoporous silica nanoparticle (E-MSN) to adsorb bacteria DNA harboring antibiotic resistance genes from wastewater at neutral pH, compared their behaviors during an investigation at different operating parameters. Meanwhile, the term chaotropic means chaos-forming in which the entropic nature of the salt can disrupt the structure of macromolecules such as protein in water, allowing the DNA in water to bind to the silica-based substance (Vandeventer et al., 2012). These chaotropic salts (sodium chloride, 2 M guanidine HCl and Urea) used in this study can disrupt the hydrogen bonding that destabilizes DNA bases and destabilizes and frees the DNA in water to facilitate binding to a silica mesopore during the adsorption process (Chen et al., 2022). The advantages of these salts used in this study include cell disruption, binding behavior to the silica surface, interfacial interactions, and can easily dissolve in water during the adsorption process. Other examples of chaotropic salts include phenol, lithium perchlorate, etc. During DNA uptake from an aqueous solution, these salts disrupt the hydrogen bonding strand of DNA and facilitate their binding onto the silica surface. This study reports on the synthesis of a type of etched MSN (E-MSN) through chemical etching techniques known as silica etched chemistry to remove the unwanted layer from the silica surface. The main reason for this procedure is to remove the hydroxyl group on the silica surface, which tends to agglomerate causing the nanoparticles to have a weak affinity (Qiao et al., 2016). Sodium dodecyl sulfate (SDS) used as an etchant was due to its high oxidizing power. This procedure was responsible for the etching of the amorphous silica framework by breaking Si–O–Si bonds, removing the OH. group and the condensed silica species and creating a new mesoporosity in the shell. It gradually etched out the negative charge electron that MSN possessed to gain electrons from other sources. This study adopted this method of synthesis in other to eliminate the negative silica surface and allows the lining of the MSN surface with chaotropic salts, which would influence the adsorption of bacteria DNA conveying ARGs onto the E-MSN mesopore.

Bacteria DNA conveying antibiotic resistance genes (bDNA-ARGs) is a public health problem of growing concern. Extensive consumption of antibiotics by humans and animals has been considered the leading cause of dissemination and proliferation of antibiotic-resistant bacteria (ARB) and ARGs detected in different water environmental bodies (Shao et al., 2018; Zainab et al., 2020). In recent decades, studies on the consequences of consuming bDNA-ARGs contaminated water and the lack of adequate treatment materials threaten public health, especially among the populace living in water-scarce areas. A study reported that ARGs enter and persist in the water environment through multiple pathways, such as sewage, domestic, agricultural, and hospital disposal (Ezeuko et al., 2021). They spread across the gut microbial communities of livestock animals, humans, and crop soil, threatening human health and ecological sustainability (Amarasiri et al., 2020; Kimbell et al., 2020). ARGs are often located at mobile genetic elements (MGEs) and spread through horizontal gene transfer (HGT) phages, plasmids, integron gene cassettes, or transposons. The release of untreated effluents containing bDNA-ARGs may prompt the indigenous bacteria to acquire ARGs through spontaneous mutation and HGT. Mutations are responsible for the continuous evolution of ARGs, producing so many variants that replicate in the water environment. The menace of bacteria DNA conveying ARGs is on the rise, increasing mortality and morbidity rates due to the lack of clean and safe water supply. Therefore, developing an efficient, less toxic material may be an excellent option to tackle the consequences of bacteria DNA conveying ARGs (bDNA-ARGs) in wastewater.

Even though there are reports on the adsorption of DNA onto MSN using multivalent cations, cationic linkers, and surface-modified MSN with functional moieties (Gao et al., 2009; Solberg and Landry, 2006; Zhang et al., 2012), to the best of our knowledge, no information on the influence of different chaotropic salts on E-MSN for the removal of bacteria DNA conveying ARGs have been published.

2. Materials and methods

2.1. Chemicals

Tetraethyl orthosilicate (TEOS), Nitric acid (HNO_3), Urea, Guanidine HCl, sodium chloride, and sodium dodecyl sulfate (SDS) were purchased from Sigma Aldrich, South Africa. Nuclease-free water and a DNA kit were purchased from Thermo Fischer. All the chemicals used in this study were of analytical grade and used as purchased.

2.2. Extraction and molecular characterization of bacterial DNA

Antibiotic-resistant *Enterococcus Faecium* used in this study was obtained from our laboratory archives isolated from the beach water in East London, Eastern Cape Province, South Africa. Before the extraction of genomic DNA, antibiotic susceptibility testing (AST) was conducted on the bacteria isolate using the disk diffusion method, following the procedure of Kirby-Bauer recommended by CLSI (Humphries et al., 2021). The result of AST confirmed that *Enterococcus Faecium* was resistant to four (5) different antibiotic drugs. They are linezolid, erythromycin, ampicillin, tetracycline, and vancomycin. Genomic DNA extraction was performed using the boiling method (Lee et al., 2020) and stored at −20 °C as a stock solution. This DNA extraction method was adopted to denature proteins, inactivate enzyme reaction inhibitors, and extract quality DNA from spots (Barbosa et al., 2016). The concentration and purity of DNA were measured by finding the absorbance ratio at 260 nm, 280 nm, and 320 nm using Multiparameter HACH DR

Table 1
PCR primers, sequences, and protocols used in this study.

Antibiotics Class	PCR primers	Primer sequences	Product size (bp)	PCR protocols	References
Tetracyclines	*tetA*	F: GCTACATCCTGCTTGCCTTC R: CATAGATCGCCGTGAAGAGG	201	94 °C–5 min; 35[94 °C–1 min; 55 °C–1 min; 72 °C 1:30 min]; 72 °C–5 min.	Titilawo et al. (2015)
	tetM	F: AGTGGAGCGATTACAGAA R: CATATGTCCTGGCGTGTCTA	158	94 °C–5 min; 35[94 °C–1 min; 55 °C–1 min; 72 °C 1:30 min]; 72 °C–5 min.	
Macrolides	*ermB*	BN1: CGAGTGAAAAAGTACTCAACA BN2: CGGTGAATATCCAAGGTACG	320	94 °C–3 min; 35 [94 °C–1 min; 55 °C–1 min; 72 °C 1 min]; 72 °C–10min.	(Adeniji et al., 2020; Osode and Okoh, 2009)

6000 Ultraviolet Spectroscopy ranging between 1.7 and 1.9, indicating that the interfering compounds were efficiently removed. A polymerase chain reaction (PCR) assay confirming the presence of resistance genes in the bacteria isolates was prepared using the primers presented in Table 1. The amplicons were examined using 1.5% (w/v) agarose gel, stained with 10 μL of ethidium bromide at a processing time of 45 min (Han et al., 2015). Then, it was pictured using the Alliance BioDoc-It system.

2.3. Synthesis and characterization of etched mesoporous silica nanoparticles (E-MSN)

E-MSN was prepared according to Salehtash et al. [11] method with slight modifications. A solution of tetraethyl orthosilicate (TEOS) in deionized water was heated to 250 °C. Nitric acid (HNO_3) was added dropwise, and the mixture was stirred at 500 rpm for 2 h to obtain a homogenous solution. Finally, urea was added slowly to the mixture. After 1 h of heating, the mixture was allowed to stir for 24 h further. Then, the mixture was calcined for 5 h at 550 °C. The calcined product was subjected to a chemical etching technique using SDS as an etchant to remove the unwanted layers and yield mesoporous materials on the synthesized materials. 3 g of SDS was dissolved in deionized water. 10 g of calcined products were added to the solution containing SDS and allowed to stir for 24 h at 80 °C. After interacting with SDS, the resulting suspension was washed several times with ethanol and water to remove the unreacted SDS. It was subjected to oven-drying for 24 h to obtain a mesoporous silica nanoparticle labeled E-MSN.

The point of zero charges (PZC) was used to determine the pH at which the net charge of the total particle surface is equal to zero or neutral. Functional groups identification, morphologies, elemental composition, and crystallinity and phase composition were determined using the Fourier transform infrared spectroscope (FTIR) (Perkin-Elmer Universal ATR 100), Scanning electron microscope (SEM) coupled with an energy dispersive x-ray spectroscope (EDX) (JOEL JSM-6390LVSEM), and X-ray diffraction (XRD) (Bruker D8) respectively.

2.4. Batch adsorption study

A batch adsorption experiment was prepared in the following procedure: 25 mL Erlenmeyer flask containing 8 mL of nuclease-free water (NSFW) was polluted with 2 mL of genomic DNA extracted from antibiotic-resistant *Enterococcus Faecium*. Adsorbents were prepared by adding 5 mg of each chaotropic salt, namely, sodium chloride (NaCl), 2 M guanidine HCl (CH_5N_3.HCl), and urea ($(NH_3)_2CO$) into 15 mg of synthesized etched mesoporous silica nanoparticles (E-MSN) labeled as E-MSN + S, E-MSN + U E-MSN + G. Then, 20 mg of each adsorbent marked as E-MSN + S, E-MSN + U, and E-MSN + G were separately weighed and added to the DNA-contaminated NFW for batch adsorption study. The effects of pH (pH range from 2 to 9 by dropwise adding 0.1 mol/L NaOH or 0.1 mol/L HCl solutions) and adsorbent dosage (ranging from 10 to 40 mg) on three adsorbents (E-MSN + S, E-MSN + U, and E-MSN + G) for bacteria DNA removal were monitored at a fixed concentration of 3.66 μg/mL, pH 7.2, contact time of 360 min and at room temperature. The experiments were conducted on a KS260 control orbital shaker at a speed of 300 rpm using a 25 mL Erlenmeyer flask with different DNA concentrations (obtained from the stock solution). After equilibration, the mixtures were subjected to centrifugal force to separate the adsorbents from the supernatant solutions. The concentrations of DNA left in the supernatant solutions were determined using a dsDNA assay kit (Q32850) Qubit 1.0 Fluorometer (Thermofischer). The percentage removal efficiency (%R) and the amount of DNA adsorbed per unit mass (qe) in all the solutions were calculated using Equations (1) and (2) described by (Ghaemi and Absalan, 2014):

Table 2
Kinetic and isotherm equations adopted in this study.

Adsorption model	Equations	Plots	References
Kinetic model	Natarajan and Khalaf first order $log\left(\frac{Ci}{Ct}\right) = \frac{K1}{2.303\,t}$ Pseudo-First order $Log\ (qe - qt) = logqe - \frac{K1}{2.303t}$ Pseudo-second order $\frac{t}{qt} = \frac{1}{K2qe2} + \frac{1}{qe}t$ Elovich model $qt = \frac{1}{\beta}\ln(\alpha\beta) + \frac{1}{\beta}\ln(t)$	$Log\left(\frac{Ci}{Ct}\right)$ *vs Time (mins)* $Log\ (qe - qt)$ *vs Time (mins)* $\frac{t}{qt}$ *vs Time (mins)* qt *vs* $\ln(t)$	Idris et al. (2012) (Karim et al., 2012; Simonin, 2016) (Idris et al., 2012; Largitte and Pasquier, 2016)
Isotherm model	Freundlich $qe = KFCe^{1/n}$ Langmuir $qe = \frac{KL\ qmCe}{1 + KLCe}$ Sips $qe = \frac{qm(KLCe)\ 1/n}{1 + (KLCe)1/n}$	qe *vs* Ce $\frac{1}{qe}$ *vs* $\frac{1}{Ce}$ qe *vs* Ce	(Uddin et al., 2017; Yusuff et al., 2019) (Ebadi and Rafati, 2015; Saman et al., 2020)

qe = μg/mg; qm = μg/mL; K_f = μg/g; K_L = mL/μg; α = $mg^{-1}\ min^{-1}$; β = μg/mg; Ce = μg/mL; Ci and Ct = μg/mL, K_1 (1/min), K_2 (g/μg min).

$$\%\mathbf{R} = \frac{(\mathbf{Ci} - \mathbf{Cf})}{\mathbf{Ci}} \times \mathbf{100} \quad (1)$$

$$\mathbf{qe} = \frac{(\ Ci - Cf\ )}{m} \times V \quad (2)$$

Where qe = the adsorption capacity at equilibrium (μg/mL), V = volume of adsorbate solution (mL), m = equal to adsorbent mass (mg), C_i and C_f are the initial and final concentrations of DNA measured in μg/mL, and % R is the removal efficiency.

2.5. Effect of contact time and adsorption kinetic

The effect of adsorption time was studied as follows: 25 mL of Erlenmeyer flask containing initial working concentrations (1.83, 3.66,

Table 3
Calculated parameter values obtained from kinetic adsorption models; K_1 and K_2 are the Natarajan and Khalaf first order, Pseudo first order, and Pseudo second-order rate constant, qe (^{cal}) and qe $^{(exp)}$ are then calculated, and experimental sorption capacity, *h,* and R^2 are the initial sorption rate related to Pseudo second order and correlation coefficient, α and β represent the initial adsorption rate and desorption constant.

Kinetic model	Adsorbents	Parameters	Initial DNA concentration (μg/mL)			
			1.83 3.66 5.49 7.32			
Natarajan and Khalaf First order	E-MSN + S	$K_1(^1/min)$	0.0000134	0.0000122	0.0000124	0.0000103
	E-MSN + U	R^2	0.73559	0.73455	0.77126	0.71712
	E-MSN + G	$K_1(^1/min)$	0.0000311	0.0000301	0.0000248	0.0000199
		R^2	0.90299	0.86761	0.81683	0.80438
		$K_1(^1/min)$	0.0000416	0.0000442	0.0000247	0.0000188
		R^2	0.92344	0.90119	0.80505	0.75812
Pseudo First Order	E-MSN + S	qe (^{cal})(μg/mg)	0.70	1.33	1.93	2.37
	E-MSN + U	K_1 (^{1}/min) qe(^{exp})(μg/mg)	0.0000446	0.0000637	0.0000644	0.0000898
	E-MSN + G	R^2	0.60	0.81	1.04	1.17
		qe (^{cal})(μg/mg)	0.88591	0.88591	0.95622	0.95493
		K_1 (^{1}/min) qe(^{exp})(μg/mg)	0.74	1.53	2.01	2.41
		qe (^{cal})R^2	0.0000647	0.0000403	0.0000483	0.0000295
		qe (^{cal})(μg/mg)	0.76	0.85	0.93	0.96
		K_1 (^{1}/min) qe(^{exp})(μg/mg)	0.9271	0.9388	0.96523	0.94332
		R^2	0.82	1.61	2.06	2.44
			0.0000743	0.0000362	0.0000391	0.0000702
			0.91	0.88	0.95	0.85
			0.97504	0.93488	0.93883	0.92852
Pseudo Second Order	E-MSN + S	qe (^{cal})(μg/mg)	0.70	1.33	1.93	2.37
	E-MSN + U	K_2 (g/μg min) qe(^{exp})(μg/mg)	1.20606	0.87374	0.72433	0.64653
	E-MSN + G	*h*	0.89	1.48	2.15	2.45
		R^2	1.47036	0.76664	0.53474	0.43124
		qe (^{cal})(μg/mg)	0.98648	0.98362	0.98824	0.99181
		K_2 (g/μg min) qe(^{exp})(μg/mg)	0.74	1.53	2.01	2.41
		h	1.17798	0.82072	0.71122	0.64547
		R^2	0.77	1.63	2.22	2.48
		qe (^{cal})(μg/mg)	1.39865	0.67916	0.51649	0.42991
		K_2 (g/μg min) qe(^{exp})(μg/mg)	0.98362	0.98765	0.99093	0.98808
		h	0.82	1.61	2.06	2.44
		R^2	1.12339	0.79202	0.70124	0.63911
			0.95	1.77	2.31	2.56
			1.26660	0.63421	0.502838	0.42196
			0.97461	0.99566	0.99677	0.99170
Elovich model	E-MSN + S	α($mg^{-1}min^1$)	1.36136	2.13191	0.69745	0.94067
	E-MSN + U	β (μg/mg)	5.49388	2.65062	0.59199	0.53406
	E-MSN + G	R^2	0.95251	0.95009	0.98972	0.99272
		α($mg^{-1}min^1$)	0.43821	1.51491	1.79431	2.39783
		β (μg/mg)	2.80432	1.89631	1.34461	1.20166
		R^2	0.95203	0.9621	0.98365	0.96081
			0.31115	1.51491	1.9668	3.19876
			1.64509	1.89631	1.35864	1.33924
			0.92575	0.96218	0.98939	0.97847

5.49, and 7.32 μg/mL obtained from stock DNA solution) at fixed pH 7.2 were in contact with 20 mg of each adsorbent labeled as E-MSN + S, E-MSN + U, and E-MSN + G at room temperature. The mixture was vortexed for 2 min and agitated using a KS260 control orbital shaker at 300 rpm for 360 min. The DNA solutions containing each adsorbent were collected at intervals ranging from 0 to 360 min. After the equilibration time, which were recorded at different time interval (180, 195, and 210 min for E-MSN + S, E-MSN + U, and E-MSN + G), the mixtures were centrifuged (PRISMER Centrifuge Labnet International) at 5000 rpm for 10 min. The final concentration of DNA residues on the supernatants was quantified.

At equilibrium time, the rate of DNA uptakes on E-MSN + S, E-MSN + U, and E-MSN + G was fitted into three (3) kinetic equations in Table 2.

2.6. Effect of initial DNA concentrations and isotherm study

Here, 20 mg of each of the three adsorbents labeled as E-MSN + S, E-MSN + U, and E-MSN + G were added to 10 mL of different initial DNA concentrations (1.83, 3.66, 5.49, and 7.32 μg/mL) at fixed pH of 7.2, and the mixtures were allowed to agitate at 300 rpm (see Table 3). Samples were collected and processed after 180, 195, and 210 min for E-MSN + S, E-MSN + U, and E-MSN + G. The initial working concentrations ranging from 1.83, 3.66, 5.49, and 7.32 μg/mL were decided using previously reported concentrations of residual DNA conveying ARGs obtained from hospital effluent (Rodriguez-Mozaz et al., 2015).

The experimental data obtained from the adsorption process involving the effect of initial DNA concentrations were fitted into three (3) isotherm models presented in Table 2.

2.7. DNA adsorption from hospital effluent using the synthesized material

The adsorption capacities of the three (3) adsorbents (E-MSN + S, E-MSN + U, and E-MSN + G) were measured in real wastewater using effluent collected from the hospital at Cofimvaba Han district municipality Queenstown, Eastern Cape Province of South Africa. The sampling was done in November 2021. The physicochemical parameters were conducted using a Multiparameter device (HANNA H19829). The hospital effluent was initially quantified to have bacteria DNA conveying ARGs. The DNA solution was used to spike hospital effluent in the ratio of 1:1, 1:2, and 1:3 to obtain 2.30, 4.13, and 5.96 μg/mL. An adsorbents dosage of 45 mg was employed at a pH of 7.29 and contact time of 180, 195, and 210 min for E-MSN + S, E-MSN + U, and E-MSN + G, respectively. All the experimental data were collected in triplicate, and the average result was used for subsequent data analysis.

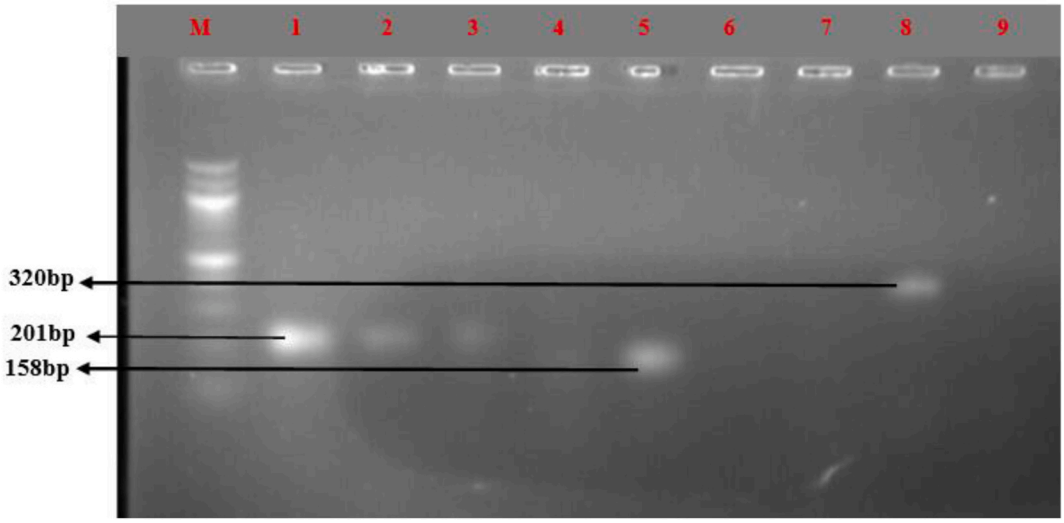

Fig. 1. Gel electrophoresis representing resistance genes for erythromycin (*ermB*) amplified at 320 bp and tetracycline (*tet*A, *tetM*) amplified at 201 and 158bp.

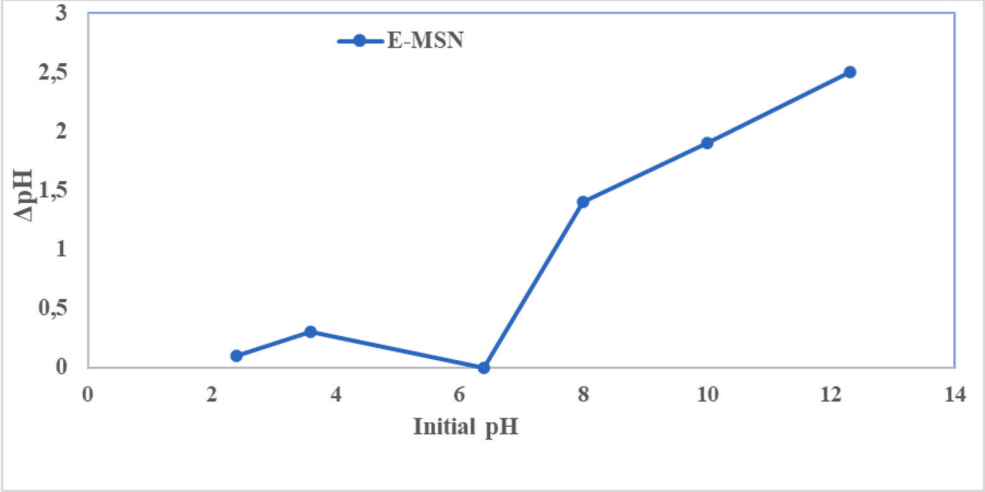

Fig. 2. Point of zero charges (PZC) of the synthesized etched mesoporous silica nanoparticles (E-MSN).

2.8. Data analysis

The data obtained from this study were plotted and analyzed using OriginPro Graphing and Analysis 2021 (v.9.8.0200), Microsoft Excel 2019, and Image J software.

3. Results and discussion

3.1. Molecular characterization of bacteria DNA from Enterococcus faecium

The amplicon or PCR product amplified at 320bp, 201bp, and 158bp for *ermB*, *tetA,* and *tetM* genes are presented in Fig. 1. The gel image shows that ***Enterococcus faecium*** harbors antibiotic-resistance genes at different base pairs.

3.2. Characterization of adsorbent (E-MSN)

3.2.1. Point of zero charges of synthesized etched mesoporous silica nanoparticles (E-MSN)

The understanding of how DNA is adsorbed onto the material surface (E-MSN) and what may be the probable arrangement was confirmed by the point of zero charges (PZC) of E-MSN. Meanwhile, PZC determines the total concentration of positive and negative control results as the surface charge equals zero. At pH > PZC, the surface charge becomes negative, while at pH < PZC, the surface charge tends to be positive (Dorigon et al., 2017). The PZC of a mesoporous silica surface is usually between 2 and 3, indicating that the hydroxyl group is protonated at a low pH value, resulting in a negative surface charge (Vilà et al., 2019). Interestingly, our result indicated the material's abnormal surface charge after silica underwent the chemical etching technique with SDS, and the PZC found was 6.3 (Fig. 2). The PZC results from this study indicated that the material's surface possesses a weak negative charge which may not be difficult for the material (E-MSN) to adsorb a large quantity of DNA by electrostatic interaction with the addition of certain salts or compounds acting as a mediator.

3.2.2. Fourier transform infrared spectroscope (FTIR) analysis

FTIR spectra presented in Fig. 3 confirmed that silica particles underwent etching chemical techniques. Successful synthesis is the evidence of IR absorption band at 462 cm^{-1}, 800 cm^{-1}, 958 cm^{-1}, and 1069 cm^{-1}. The band at 462 cm^{-1} indicated the Si–O bending mode at 805 $cm^{-1,}$ and 1069 cm^{-1} confirmed the asymmetric and symmetric stretching of the Si–O–Si bridge, and the obscure band at 997 cm^{-1}

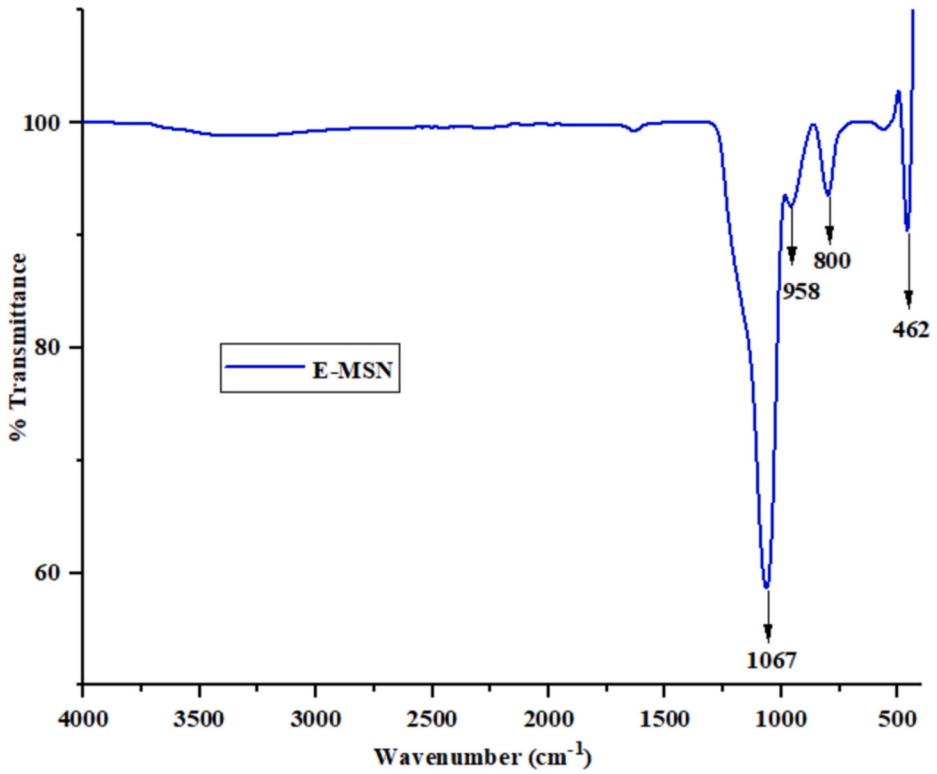

Fig. 3. FTIR spectra of mesoporous silica nanoparticles synthesized by a chemical etching technique.

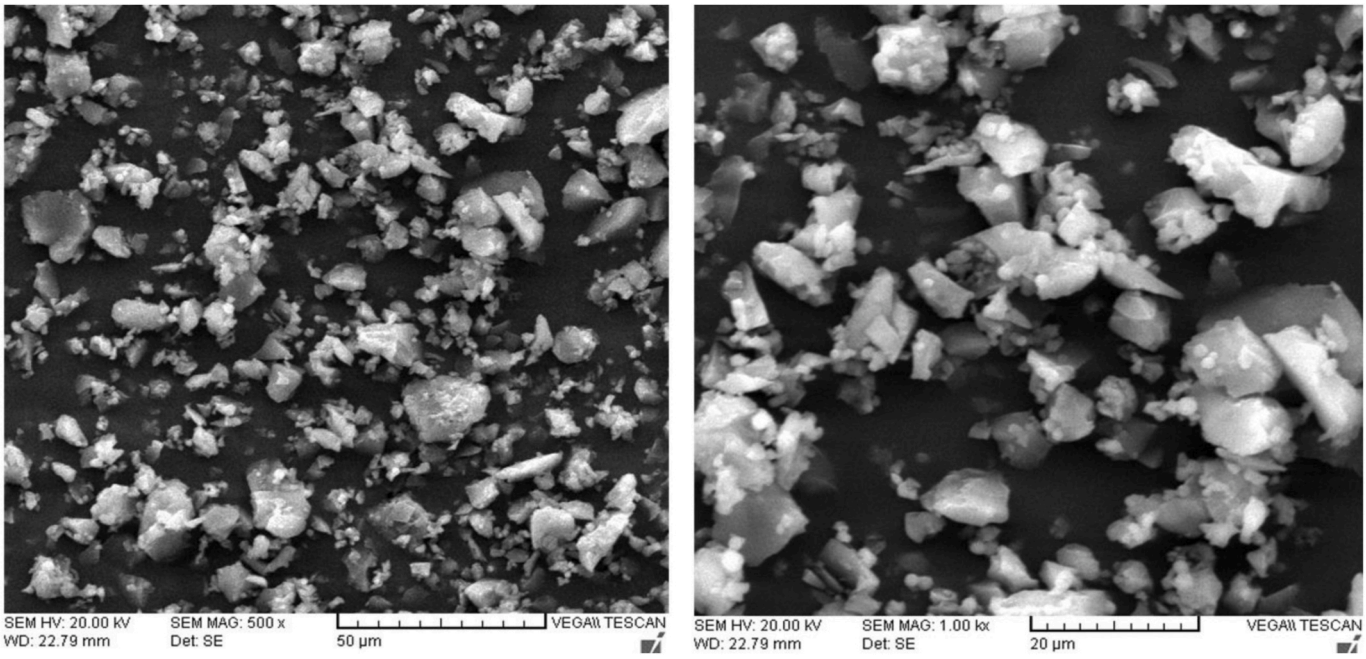

Fig. 4. A and B: SEM images of E-MSN at high (A = 50 µm) and low (B = 20 µm) magnifications showing non-spherical morphology and less agglomerated particles.

corresponded to the Si–OH group. The spectra obtained are similar to MSN synthesized through the chemical etching technique (Jabir et al., 2018; Salehtash et al., 2018). The FTIR result shows no SDS on the E-MSN surface, showing that subsequent washing by ethanol and water for SDS removal was effective.

3.2.3. Scanning electron microscope (SEM) analysis

SEM investigated the morphology of E-MSN. As indicated in Fig. 4a and b, the E-MSN captured in different magnifications (20 µm and 50 µm) showed a non-spherical shape with nearly uniform size and formation of agglomeration. The particles' surface was rough, which may be attributed to surface pore formation (Jia et al., 2013). Agglomeration of E-MSN may be attributed to the chemical etching technique used during the synthesis and may occur due to removing unwanted layers from the material. The SEM image is similar to previously published reports on the synthesis of MSN through chemical etching chemistry

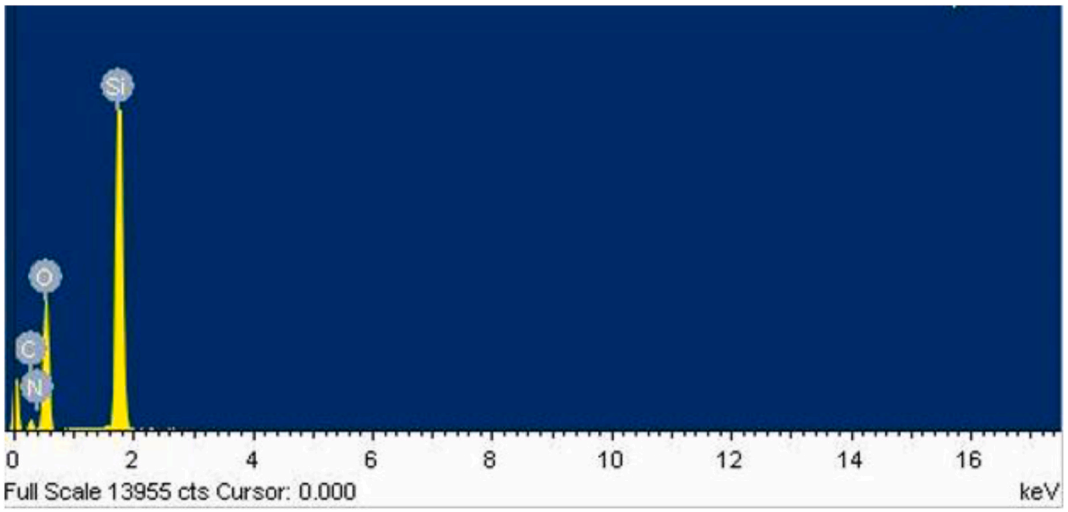

Fig. 5. Energy-dispersive X-ray spectroscopy (EDX) of synthesized E-MSN showing a strong signal of silica (Si) at approximately 2 Kev.

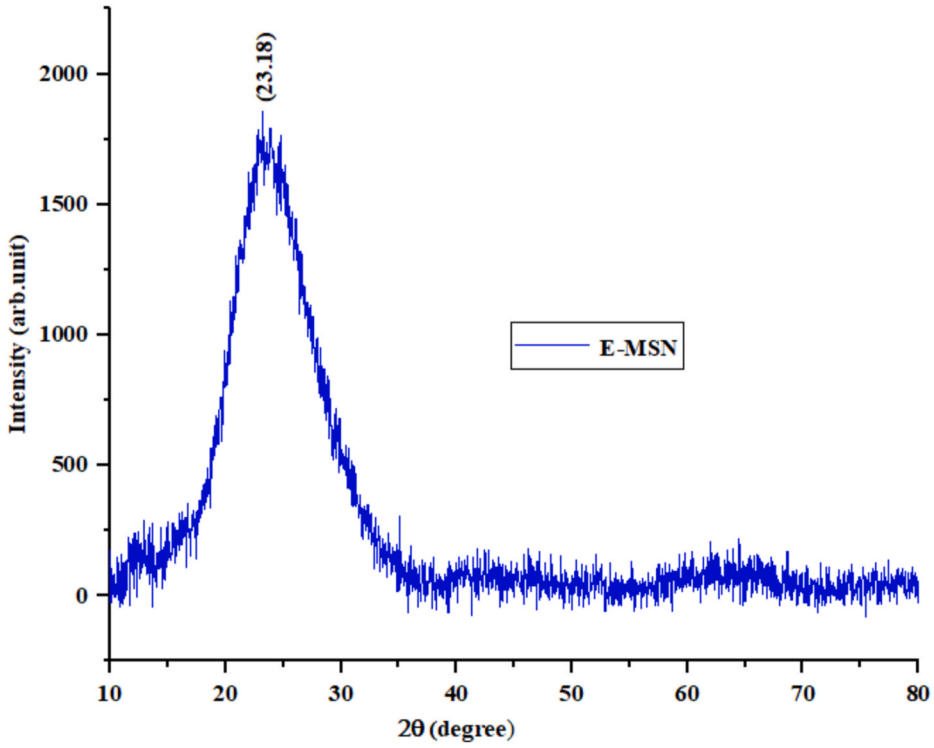

Fig. 6. Typical XRD pattern of synthesized silica etched mesoporous nanoparticle (E-MSN).

(Salehtash et al., 2018).

3.2.4. Energy dispersive x-ray spectroscope (EDX) analysis

EDX determined the elemental composition of E-MSN. Fig. 5 showed a strong signal from the silica (Si) region at approximately 2 Kev with 31.12% weight. Other elements detected at weak signals are carbon (C), oxygen (O), and nitrogen (N) at 17.44%, 46.75%, and 4.46%, respectively. With their % compositions, these elements confirmed the material (E-MSN) purity. The result is similar to previously reported studies (Salehtash et al., 2018; Saman et al., 2020).

3.2.5. X-ray diffraction (XRD) analysis

The X-ray diffraction pattern determined the average crystalline structure of the synthesized E-MSN. Fig. 6 shows the evidence that particles are crystalline. The intense peak at $\theta = 23.18^{o}$ confirmed the evidence of silica nanoparticles in the amorphous state. The intense peak showed the high purity of the material (E-MSN). Due to more negligible particle size effects, incomplete inner structure, and regular periodic variation of electron density occur during the ordering of pores in mesoporous silica nanoparticles (Sharmiladevi et al., 2016). Also, the intense peak can be indexed to the hexagonal lattice structure related to the mesoporous silica net (Soares et al., 2015).

3.3. Studies on the operating parameters for the adsorption process

3.3.1. pH effect on bacteria DNA adsorption

Varying the pH of the DNA solution plays a vital role in determining adsorption capacity, the efficiency of the adsorbent's surface charge,

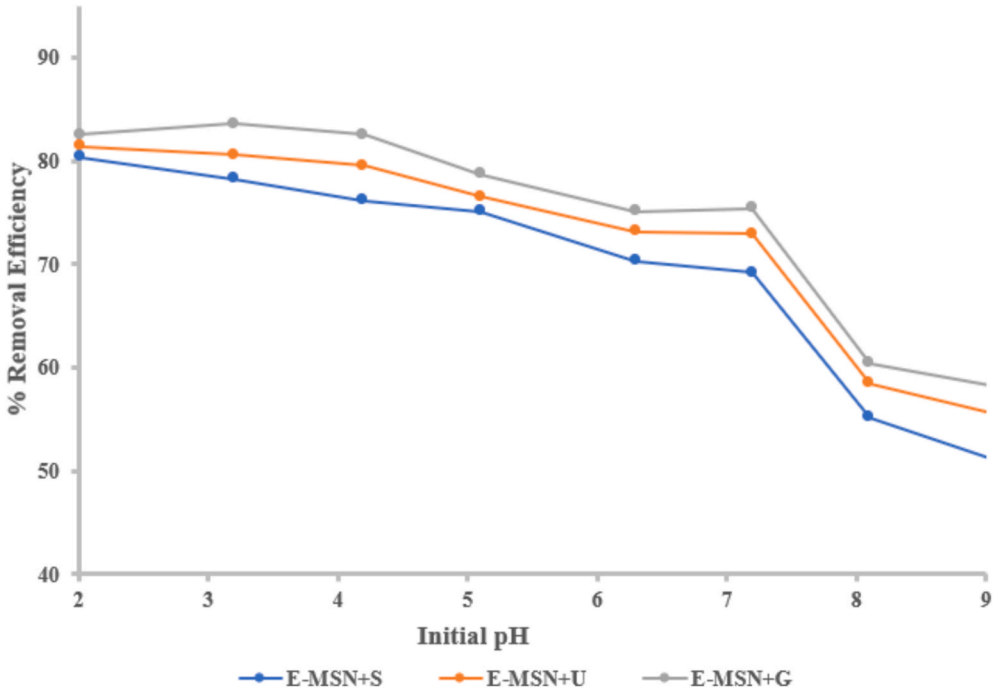

Fig. 7. Effect of pH on the removal efficiency of DNA; adsorbent dose = 20 mg, adsorbate concentration = 3.66 μg/mL, reaction time = 360 min and speed = 300 rpm and at room temperature.

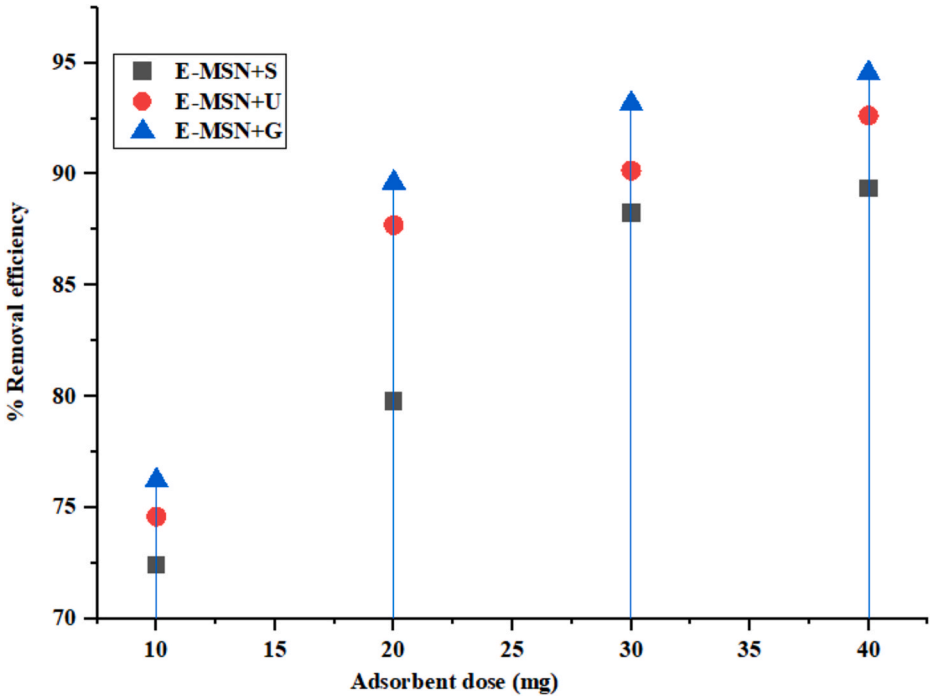

Fig. 8. Effect of adsorbent dose on the removal of bacteria DNA onto E-MSN + S, E-MSN + U, and E-MSN + G, adsorbate concentration = 3.66 μg/mL, reaction time = 180, 195, and 210 min; Speed = 300 rpm, pH = 7.2, and at room temperature.

and the adsorbate molecules' ionization state (Aarab et al., 2020). The effects of pH on bacteria DNA removal by the three (3) adsorbents labeled as E-MSN + S, E-MSN + U, and E-MSN + G were studied over a wide range, pH values 2 to 9, with the initial concentration of 3.66 μg/mL, contact time of 0–360 min and at a fixed adsorbents dosage of 20 mg of each adsorbent. The experiment was conducted at room temperature, with a speed of 300 rpm, and the results were captured in Fig. 7. It was observed that, at acidic pH (2-6), the removal efficiencies increased above 80% in all the adsorbents. This was due to the deprotonation of DNA molecules, and the protonation of functional groups (guanidinium, amine, carbonyl, Na+, and Cl-) found in the adsorbents promotes electrostatic attraction between the negative charge of DNA and positively charged surface adsorbents (He et al., 2020). The adsorption of bacteria DNA onto the adsorbents decreased drastically to 55–60% at basic pH (8–9). This may be attributed to the competition between O.H.ˉ ions and deprotonated DNA molecules in the adsorption

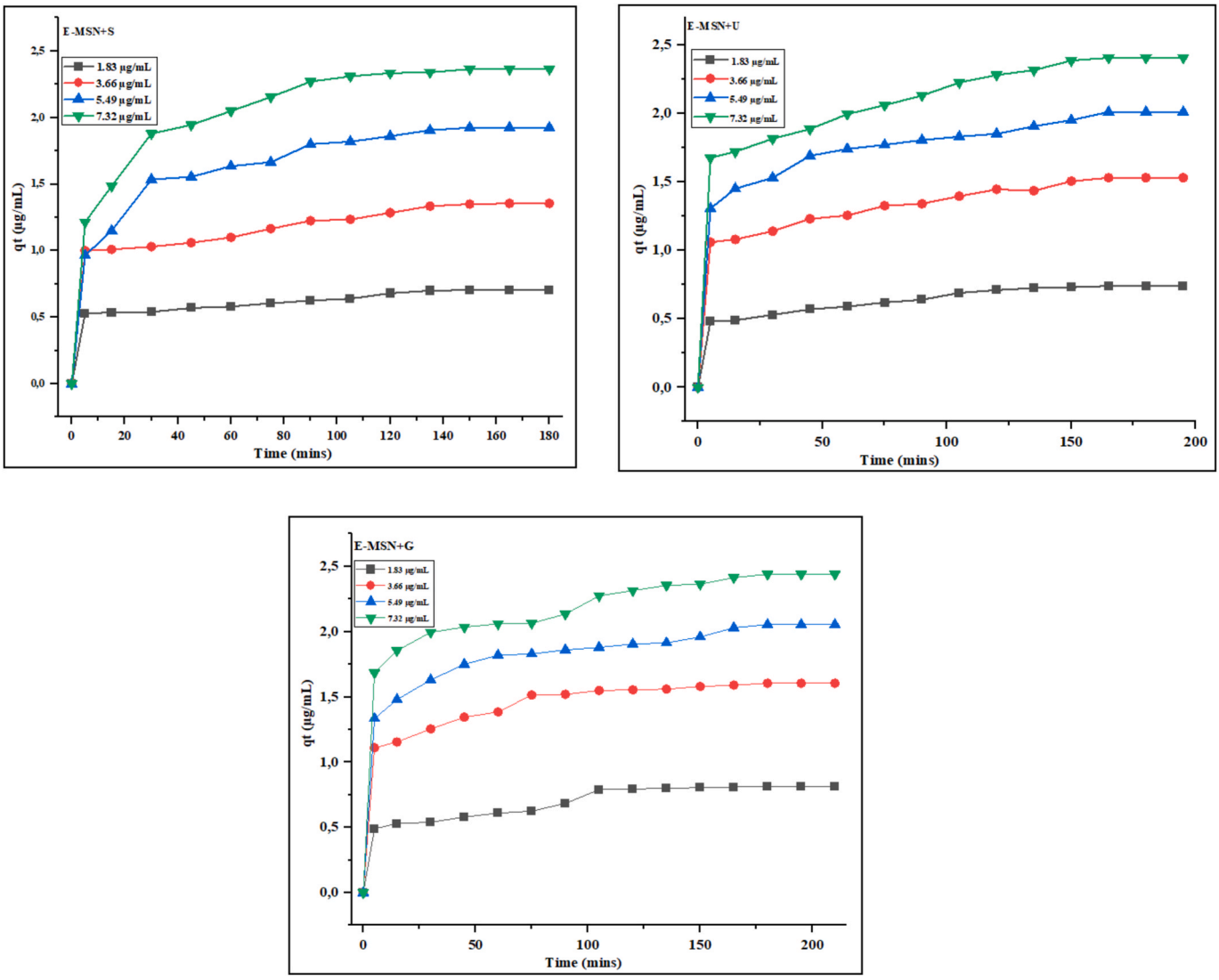

Fig. 9. ARepresent the effect of contact time for E-MSN + S, E-MSN + U and E-MSN + G at different adsorbate concentrations (1.83, 3.66, 5.49 and 7.32 µg/mL); reaction time of 180, 195, and 210 min, sorbent dose = 20 mg, speed = 300 rpm, and pH = 7.2 at room temperature.

site (El-Bindary et al., 2018). Meanwhile, at neutral pH (7.2), the removal efficiencies for E-MSN + S, E-MSN + U, and E-MSN + G were 70%, 73%, and 76%. The optimum pH for DNA adsorption onto E-MSN + S, E-MSN + U, and E-MSN + G was pH 2.01. This study, pH 7.2 was considered for further experimental analysis because DNA bases remain intact at neutral pH without any interference from either acid-based solution or external factors.

3.3.2. *Sorbent effects on bacteria DNA adsorption*

The sorbent dose is essential in determining an adsorbent's sorption capacity for a given initial concentration during the adsorption process (Batool et al., 2018). In this study, the adsorbent mass on the DNA adsorption was studied and illustrated in Fig. 8. The result obtained complied with an already published article on DNA adsorption onto ultrathin nanosheets (Wang et al., 2014). The etched MSN combined with the chaotropic salts (adsorbents) was adequate compared to the adsorption of bacterial DNA onto ordinary MSN. This is because synthesizing the adsorbent (etched MSN) assisted in shredding the repulsion effects that may occur between the negative silica surface and the negative contaminant (since DNA is highly negative in its backbone). As expected, the percentage removal of bacteria DNA rapidly increased with an increase in sorbent mass from 10 to 40 mg. At 40 mg, the optimum removal efficiencies reached 89%, 92%, and 94% for E-MSN + S, E-MSN + U, and E-MSN + G, respectively. We observed that removal efficiencies increased in the following order: E-MSN + G > E-MSN + U > E-MSN + S by increasing the adsorbent dose to 40 mg. The high removal efficiency of E-MSN + G is attributed to the protonation of guanidine HCl, producing a more positive charge on the adsorbent's surface, thus increasing electrostatic interaction between the DNA and the sorbent. More surface-active sites were available for the bacteria DNA to penetrate easily into the sorption site (Bundjaja et al., 2021). To obtain a constant value, the sorbent dose was increased to 50 mg at fixed initial concentrations of 3.66 µg/mL of the DNA solution; the value obtained showed no significant removal of DNA adsorbed onto the adsorbents. Therefore, an adsorbent dose of 40 mg was chosen for further studies.

3.4. *Effect of contact time and kinetics study*

This study studied the effect of contact time because it reflected the adsorption kinetics of an adsorbent for a given concentration of DNA solution. It determines the adsorbent's efficiency in the adsorption of pollutants from wastewater through rapid uptake of the adsorbate (Chen et al., 2019). The effect of contact time on the adsorption of bacteria

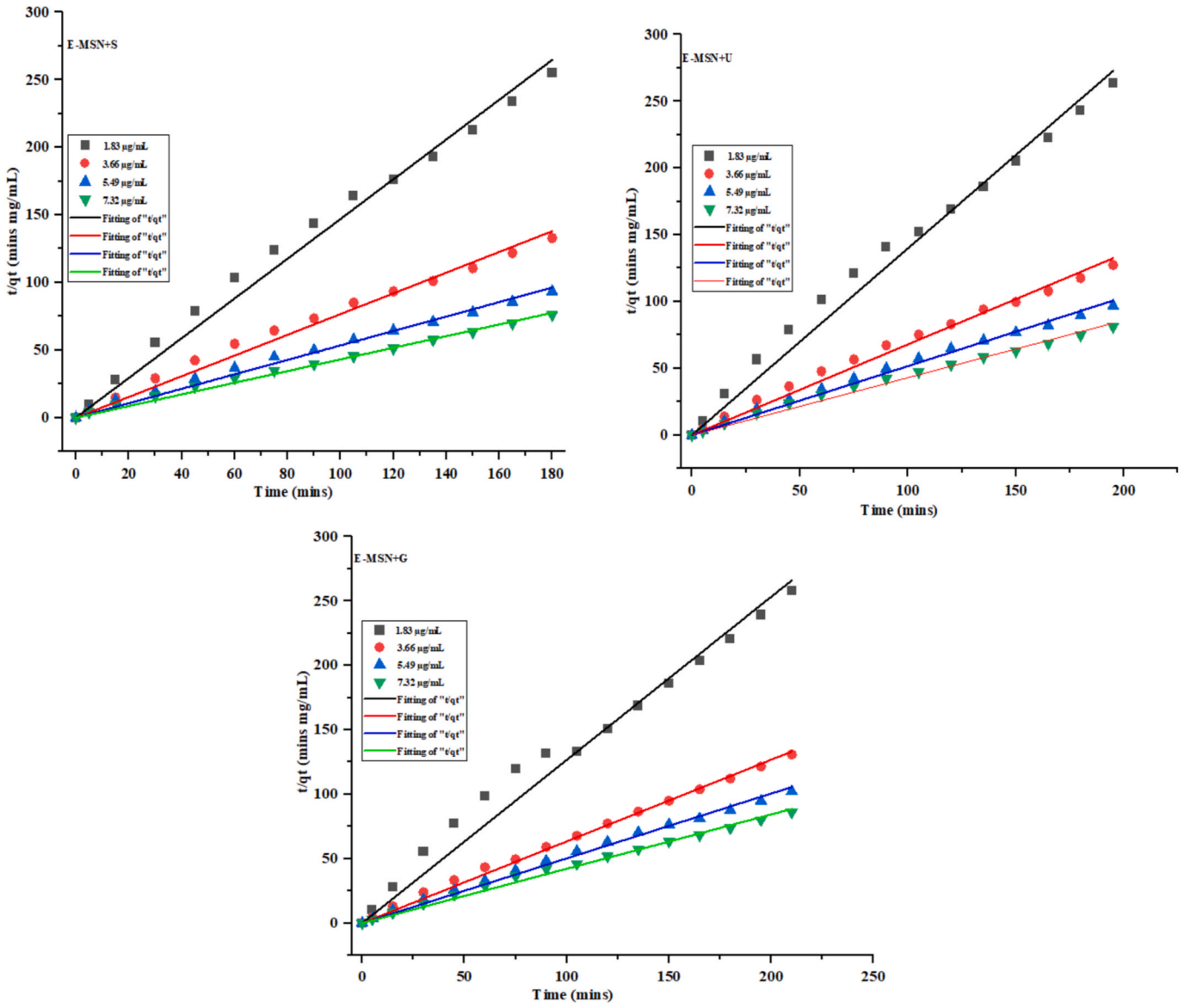

Fig. 9. BThe kinetic of the nonlinear plot of the pseudo-second-order model for DNA adsorption onto E-MSN + S, E-MSN + U, and E-MSN + G.

DNA onto the adsorbents (E-MSN + S, E-MSN + U, and E-MSN + G) at different initial concentrations (1.83, 3.66, 5.49, and 7.32 μg/mL) are shown in Fig. 9A. The result showed that the adsorption capacity of bacteria DNA on the E-MSN + S, E-MSN + U, and E-MSN + G was rapid between 5 and 15 min at different initial concentrations and gradually stagnated with the increase in contact time. We noticed that equilibration time for DNA adsorption occurred at 180, 195, and 210 min for E-MSN + S, E-MSN + U, and E-MSN + G, respectively. Adsorption capacity obtained at each adsorbent increased simultaneously in the order of E-MSN + G >E-MSN + U > E-MSN + S. The increase in adsorption capacity within 5–15 min is attributed to the availability of positively surface-charged E-MSN enhanced by the chaotropic salt. At the same time, the gradual process of reaching the equilibrium time could be slow pore diffusion of DNA molecules into the bulk of the adsorbents. However, we observed that the adsorption capacity measured by the adsorbents reduces at an increase in concentrations of DNA solution. It is because high adsorption capacity is highly dependent on the initial concentrations of DNA.

To study the adsorption kinetics of the experimental data obtained from E-MSN + S, E-MSN + U, and E-MSN + G, four (4) kinetic models, namely, Natarajan and Khalaf first order (NKFO), Pseudo-First order (PFO), Pseudo-second order (PSO), and Elovich model equations were applied to the adsorption data. The results of kinetic parameters obtained are shown in Table 2; where K_1 (min^{-1}), K_2 (μg/mL mins), β (μg/mg), and α (mg^{-1} min^{-1}) are the equilibrium NKFO, PFO, PSO, and Elovich model rate constants respectively. According to Table 2 and Fig. 9B, pseudo-second-order exhibited the highest correlation coefficient (R^2 ranging from 0.97 to 0.99 for E-MSN + S, E-MSN + U, and E-MSN + G) than other kinetic models investigated. The highest R^2 values exhibited by PSO confirmed the kinetic mechanism of adsorption onto E-MSN + S, E-MSN + U, and E-MSN + G was based on chemisorption, which involved electron sharing between DNA molecules and the adsorbent's surface charge. Also, the calculated qe (qe cal) equilibrium values were closely related to the qe experimental (qe ^{exp}). This confirmed that PSO correlated with DNA adsorption onto surface-enhanced mesoporous silica nanoparticles (E-MSN + S, E-MSN + U, and E-MSN + G). To further confirm the authenticity of pseudo-second-order as the best fit for this study, the initial sorption rate was calculated using equation (3):

$$h = K2 \times qe2 \tag{3}$$

The value of *h* obtained from initial DNA concentrations decreases in

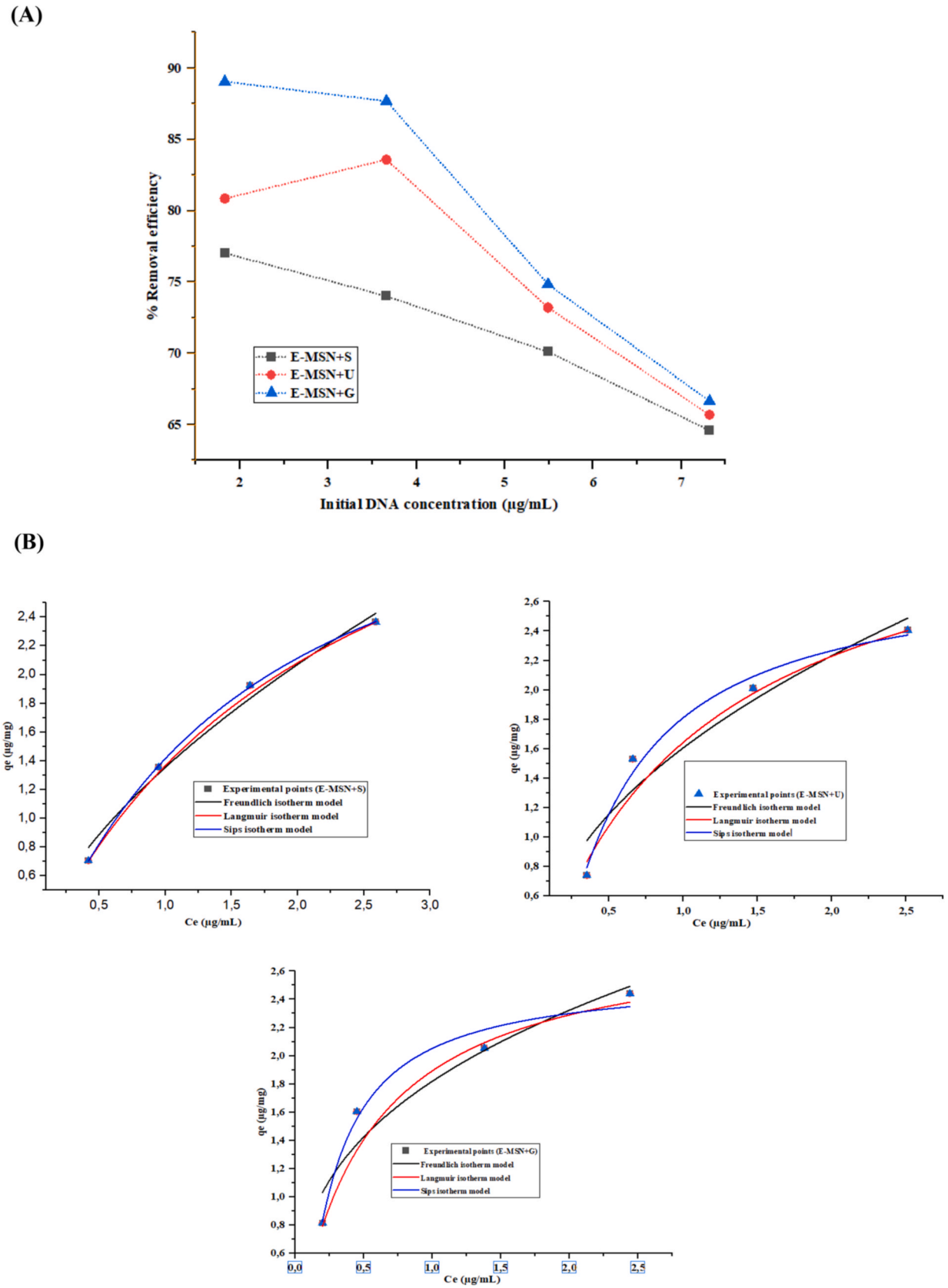

Fig. 10. (A) Effects of DNA initial concentration on adsorption process; (B) Nonlinear plots of Langmuir, Freundlich, and Sips isotherm model.

Table 4
Isotherm parameters for the adsorption of bacteria DNA (ARGs) onto E-MSN + S, E-MSN + U, and E-MSN + G at room temperature.

Isotherm	Parameter	E-MSN + S	E-MSN + U	E-MSN + G
Langmuir	qmax (μg/mL)	4.3792	3.4614	2.896
	$K_{L.}$ (μg/g)	0.4532	0.9045	1.887
	$R_{L.}$	0.5466	0.3766	0.225
	X^2	0.0012	0.0024	0.0050
	R^2	0.9794	0.9865	0.9673
Freundlich	K_f (μg/g)	1.3545	1.6068	1.8194
Sips	n	1.6319	2.1071	2.8351
	X^2	0.0111	0.0567	0.0519
	R^2	0.9557	0.9263	0.9297
	qmax	3.8281	2.8373	2.5775
	Ks	0.7886	2.4059	4.4167
	n	1.2265	1.0818	1.1281
	X^2	0.002	0.018	0.028
	R^2	0.9998	0.9879	0.98971

the same order as K_2, indicating a low adsorption rate at the increase in initial DNA concentration.

3.5. Effect of initial concentrations and isotherm study

The plots of E-MSN + S, E-MSN + U, and E-MSN + G percentage removal efficiency against initial concentrations are presented in Fig. 10A. In all three adsorbents, it was observed that the amount of DNA adsorbed onto sorbent mass decreased with the increase in the initial concentrations (1.83, 3.66, 5.49, and 7.32 μg/mL). At equilibrium, the percentage (%) removal efficiencies obtained from each adsorbent are 70.04, 74.04, 70.12 and 64.61 (E-MSN + S); 80.87, 83.60, 73.22, and 65.71 (E-MSN + U); and 89.07, 87.70, 74.86, and 66.66 (E-MSN + G). From the results, E-MSN + G exhibited the highest performance in removing DNA conveying ARGs followed by E-MSN + U and E-MSN + S. Generally, the decrease in removal efficiencies of E-MSN + S and E-MSN + U compared to the literature may be attributed to the adsorptive site being saturated due to an increase in initial concentrations of DNA. Also, the materials' inability to produce a more positive charge would facilitate the adsorption of DNA onto the adsorbents at the increase in adsorbate concentration. Therefore, to describe the transmission of DNA from the solution phase to the adsorbent phase at equilibrium conditions, adsorption isotherms such as Freundlich, Langmuir, and Sips models were used to evaluate the experimental data. Generally, the Freundlich model is best fitted when adsorption occurs on a heterogeneous surface, having unequal active sites and different energies of adsorption (Al-Ghouti and Da'ana, 2020; Yang et al., 2021). The Langmuir model applies the adsorption at the specific homogenous sites within the adsorbent, forming a single layer over the surface of the adsorbent (Miyah et al., 2018; Panão et al., 2019). The Sips model, a three-parameter isotherm, describes a combination of Freundlich and Langmuir models. The model is suitable for adsorption on a heterogeneous surface, avoiding the limitations of increased adsorbate concentration normally associated with the Freundlich model (Kumar et al., 2019; Siqueira et al., 2020). Therefore, this model concluded that at a low adsorbate concentration, Freundlich is predicted, but it depicts Langmuir at a high adsorbate concentration (Ayawei et al., 2017). The given equation for the three isotherm models (Table 1) was plotted (Fig. 10B), and the values obtained were evaluated from the slope and intercept of nonlinear plots (Table 4). The three-parameter adsorption model (Sips) obtained from the experimental values reasonably agrees with DNA adsorption onto E-MSN + S, E-MSN + U, and E-MSN + G. The adsorption data obtained from all the three adsorbents were best well fitted into Sips model (R^2 = 0.99982, 0.98798, and 0.98971 for E-MSN + S, E-MSN + U and E-MSN + G) with reduced Chi-square (0.002, 0.01, and 0.02) than Freundlich (R^2 = 0.95571, 0.92632, and 0.92971) and Langmuir (R^2 = 0.979418, 0.98645, and 0.96727). The highest R^2 values obtained from the sips model indicated that DNA adsorption onto E-MSN + S, E-MSN + U, and E-MSN + G was achieved via heterogeneous surfaces.

Table 5
Physicochemical parameters of hospital wastewater.

pH	Temperature	Total dissolved solids	Dissolved oxygen	Turbidity	Initial DNA concentration in wastewater (μg/mL)
7.79	13.35	30	7.29	15.9	0.474

Although the maximum % removal obtained from E-MSN + S (77.04) and E-MSN + U (80.8) is lower than the value (89.5%) reported in the literature for DNA adsorption onto magnetic silica surface (Li et al., 2012); they are still advantageous because DNA can adsorbed onto the mesopore of silica nanoparticles by addition of chaotropic salts alongside the adsorbent without any costly modification. It can be quickly recovered from the treated water. These characteristics make E-MSN + S, E-MSN + U, and E-MSN + G an economical option that can tackle bacteria DNA menace across the globe.

3.6. Proof of concept (removal of bacterial DNA from hospital wastewater)

To ascertain the effectiveness of E-MSN + S, E-MSN + U, and E-MSN + G in a real-life scenario, real hospital wastewater was collected from Cofimvaba Han district Queenstown, Eastern Cape province of South Africa. The physicochemical parameters obtained before the commencement of the study are presented in Table 5. The result of the physicochemical analysis showed that hospital effluent is in a toxic condition with moderate total dissolved solids. After spiking to obtain different initial working concentrations, the concentration of bacteria DNA was subjected to a batch adsorption study. At optimum conditions, the maximum % adsorption efficiency obtained at different initial concentrations (2.3, 4.13, and 5.96 μg/mL) were in the range of 60–71%, 63–73%, and 76–94% for E-MSN + S, E-MSN + U and E-MSN + G respectively (Fig. 11). It was observed that the % adsorption efficiency obtained from real hospital wastewater is lower than the simulated water. This may be attributed to other anionic interference present in the real wastewater. The anionic interference may cause repulsion effects between DNA molecules and adsorbents at the adsorptive site. The result indicated that E-MSN + G showed high removal efficiency of bacteria DNA conveying ARGs from hospital wastewater.

4. Conclusion

The etched mesoporous silica nanoparticles were successfully synthesized via chemical etching techniques. The synthesized material was enhanced with different chaotropic salts to obtain E-MSN + S, E-MSN + U, and E-MSN + G, and the applications were extended to hospital wastewater to remove bacteria DNA conveying ARGs. The result showed that DNA could bind onto the mesopore of silica nanoparticles with the help of different chaotropic salts. E-MSN + G exhibited high removal efficiency in adsorbing bacteria DNA conveying ARGs in simulated water and hospital wastewater. Moreover, the adsorbents exhibited high adsorption capacities and dispersibility and were easily recovered from an aqueous solution. The study batch adsorption parameters (effects of solution pH, contact time, adsorbent dosage, and initial concentrations) contributed significantly to the uptake of DNA from water/wastewater. The kinetics and isotherm studies of the experimental data fitted well into pseudo-second-order and Sips models, respectively. The adsorption isotherm model suggests heterogenous chemisorption for DNA uptake onto E-MSN + S, E-MSN + U, and E-MSN + G. Therefore, synthesized material aided by the different chaotropic salts (E-MSN + S, E-MSN + U, and E-MSN + G) showed high performance and can be an effective material for removing bacteria DNA from hospital wastewater.

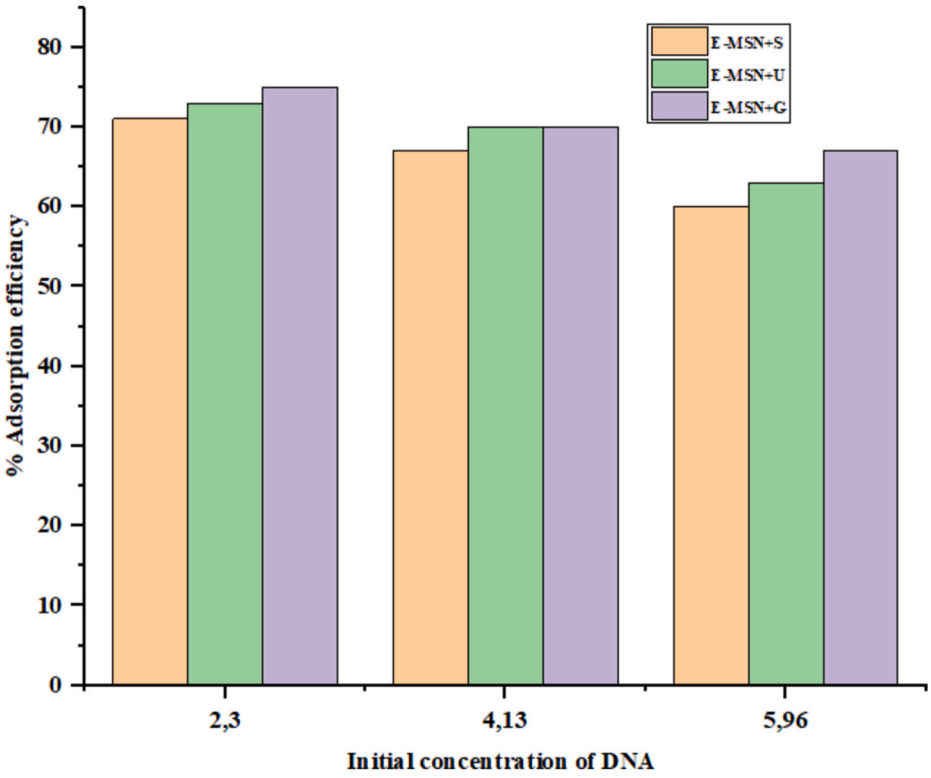

Fig. 11. The removal of bacteria DNA conveying ARG from hospital wastewater.

CRediT authorship contribution statement

Adaora S. Ezeuko: Writing – original draft, Funding acquisition, conducted the research and finalized the draft of the manuscript. **Mike O. Ojemaye:** Writing – original draft, Supervision, Funding acquisition, supervised and fine-tuned the different drafts of this manuscript. **Omobola O. Okoh:** Writing – original draft, Supervision, Funding acquisition, supervised and fine-tuned the different drafts of this manuscript. **Anthony I. Okoh:** Funding acquisition, the study's advisor and provided funding during the manuscript writing.

Declaration of competing interest

The authors declare that they have no known competing financial interests or personal relationships that could have appeared to influence the work reported in this paper.

Data availability

Data will be made available on request.

Acknowledgments

The authors thank the South Africa Medical Research Council for financial support.

References

Aarab, N., Hsini, A., Essekri, A., Laabd, M., Lakhmiri, R., Albourine, A., 2020. Removal of an emerging pharmaceutical pollutant (metronidazole) using PPY-PANi copolymer: kinetics, equilibrium and DFT identification of adsorption mechanism. Groundw. Sustain. Dev. 11 https://doi.org/10.1016/j.gsd.2020.100416.

Abbaraju, P.L., Pharm, B., Pharm, M., 2009. Mesoporous Silica Nanoparticles for Biomedical Applications.

Adeniji, O.O., Sibanda, T., Okoh, A.I., 2020. Molecular detection of antibiotic resistance and virulence gene determinants of Enterococcus species isolated from coastal water in the Eastern Cape Province, South Africa. Int. J. Environ. Stud. 1–20 https://doi.org/10.1080/00207233.2020.1785759.

Al-Ghouti, M.A., Da'ana, D.A., 2020. Guidelines for the use and interpretation of adsorption isotherm models: a review. J. Hazard Mater. https://doi.org/10.1016/j.jhazmat.2020.122383.

Amarasiri, M., Sano, D., Suzuki, S., 2020. Understanding human health risks caused by antibiotic resistant bacteria (ARB) and antibiotic resistance genes (ARG) in water environments: current knowledge and questions to be answered. Crit. Rev. Environ. Sci. Technol. 50, 2016–2059. https://doi.org/10.1080/10643389.2019.1692611.

Ayawei, N., Ebelegi, A.N., Wankasi, D., 2017. Modelling and interpretation of adsorption isotherms. J. Chem. https://doi.org/10.1155/2017/3039817, 2017.

Barbosa, C., Nogueira, S., Gadanho, M., Chaves, S., 2016. DNA Extraction: Finding the Most Suitable Method, Molecular Microbial Diagnostic Methods: Pathways to Implementation for the Food and Water Industries. Elsevier Inc. https://doi.org/10.1016/B978-0-12-416999-9.00007-1.

Batool, F., Akbar, J., Iqbal, S., Noreen, S., Bukhari, S.N.A., 2018. Study of isothermal, kinetic, and thermodynamic parameters for adsorption of cadmium: an overview of linear and nonlinear approach and error analysis. Bioinorgan. Chem. Appl. https://doi.org/10.1155/2018/3463724, 2018.

Bundjaja, V., Santoso, S.P., Angkawijaya, A.E., Yuliana, M., Soetaredjo, F.E., Ismadji, S., Ayucitra, A., Gunarto, C., Ju, Y.H., Ho, M.H., 2021. Fabrication of cellulose carbamate hydrogel-dressing with rarasaponin surfactant for enhancing adsorption of silver nanoparticles and antibacterial activity. Mater. Sci. Eng. C. https://doi.org/10.1016/j.msec.2020.111542.

Chen, B., Zhao, H., Chen, S., Long, F., Huang, B., Yang, B., Pan, X., 2019. A magnetically recyclable chitosan composite adsorbent functionalized with EDTA for simultaneous capture of anionic dye and heavy metals in complex wastewater. Chem. Eng. J. 356, 69–80. https://doi.org/10.1016/j.cej.2018.08.222.

Chen, J., Peng, Q., Peng, X., Zhang, H., Zeng, H., 2022. Probing and manipulating noncovalent interactions in functional polymeric systems. Chem. Rev. https://doi.org/10.1021/acs.chemrev.2c00215.

de Greñu, B.D., de los Reyes, R., Costero, A.M., Amorós, P., Ros-Lis, J.V., 2020. Recent progress of microwave-assisted synthesis of silica materials. Nanomaterials 10, 1–21. https://doi.org/10.3390/nano10061092.

Dorigon, L., Ruiz de Almeida da Frota, J.P., Kreutz, J.C., Mello Giona, R., Pereira Moisés, M., Bail, A., 2017. Synthesis and characterization of mesoporous silica-coated magnetite containing cetyltrimethylammonium bromide and evaluation on the adsorption of sodium dodecylbenzenesulfonate. Appl. Surf. Sci. 420, 954–962. https://doi.org/10.1016/j.apsusc.2017.05.249.

Ebadi, A., Rafati, A.A., 2015. Preparation of silica mesoporous nanoparticles functionalized with β-cyclodextrin and its application for methylene blue removal. J. Mol. Liq. 209, 239–245. https://doi.org/10.1016/j.molliq.2015.06.009.

El-Bindary, M.A., El-Deen, I.M., Shoair, A.F., 2018. Removal of anionic dye from aqueous solution using magnetic sodium alginate beads. J. Mater. Environ. Sci. 10, 604–617.

Ezeuko, A.S., Ojemaye, M.O., Okoh, O.O., Okoh, A.I., 2021. Technological advancement for eliminating antibiotic resistance genes from wastewater: a review of their

mechanisms and progress. J. Environ. Chem. Eng. https://doi.org/10.1016/j.jece.2021.106183.
Gao, F., Botella, P., Corma, A., Blesa, J., Dong, L., 2009. Monodispersed mesoporous silica nanoparticles with very large pores for enhanced adsorption and release of DNA. J. Phys. Chem. B 113, 1796–1804. https://doi.org/10.1021/jp807956r.
Ghaemi, M., Absalan, G., 2014. Study on the adsorption of DNA on Fe3O4 nanoparticles and on ionic liquid-modified Fe3O4 nanoparticles. Microchim. Acta 181, 45–53. https://doi.org/10.1007/s00604-013-1040-5.
Han, J.E., Mohney, L.L., Tang, K.F.J., Pantoja, C.R., Lightner, D.V., 2015. Plasmid mediated tetracycline resistance of Vibrio parahaemolyticus associated with acute hepatopancreatic necrosis disease (AHPND) in shrimps. Aquac. Reports. https://doi.org/10.1016/j.aqrep.2015.04.003.
He, Q., Wu, Q., Feng, X., Liao, Z., Peng, W., Liu, Y., Peng, D., Liu, Z., Mo, M., 2020. Interfacing DNA with nanoparticles: surface science and its applications in biosensing. Int. J. Biol. Macromol. 151, 757–780. https://doi.org/10.1016/j.ijbiomac.2020.02.217.
Humphries, R., Bobenchik, A.M., Hindler, J.A., Schuetz, A.N., 2021. Overview of changes to the clinical and laboratory standards institute performance standards for antimicrobial susceptibility testing, M100, 31st edition. J. Clin. Microbiol. 59, e0021321 https://doi.org/10.1128/JCM.00213-21.
Idris, S., Iyaka, Y.A., Ndamitso, M.M., Mohammed, E.B., Umar, M.T., 2012. Evaluation of kinetic models of copper and lead uptake from dye wastewater by activated pride of Barbados shell. Am. J. Chem. 1, 47–51. https://doi.org/10.5923/j.chemistry.20110102.10.
Jabir, M.S., Nayef, U.M., Jawad, K.H., Taqi, Z.J., Buthenhia, H., Ahmed, N.R., 2018. Porous silicon nanoparticles prepared via an improved method: a developing strategy for a successful antimicrobial agent against Escherichia coli and Staphylococcus aureus. IOP Conf. Ser. Mater. Sci. Eng. 454 https://doi.org/10.1088/1757-899X/454/1/012077.
Jafari, S., Derakhshankhah, H., Alaei, L., Fattahi, A., 2018. Biomedicine & Pharmacotherapy Mesoporous silica nanoparticles for therapeutic/diagnostic applications. Biomed. Pharmacother. 109, 1100–1111.
Jia, L., Shen, J., Li, Z., Zhang, D., Zhang, Q., Liu, G., Zheng, D., Tian, X., 2013. In vitro and in vivo evaluation of paclitaxel-loaded mesoporous silica nanoparticles with three pore sizes. Int. J. Pharm. 445, 12–19. https://doi.org/10.1016/j.ijpharm.2013.01.058.
Jiang, H., Guo, Y., Wei, C., Hu, P., Shi, J., 2021. Nanocatalytic innate immunity activation by mitochondrial DNA oxidative damage for tumor-specific therapy. Adv. Mater. 33, 1–11. https://doi.org/10.1002/adma.202008065.
Kankala, R.K., Han, Y.H., Na, J., Lee, C.H., Sun, Z., Wang, S. Bin, Kimura, T., Ok, Y.S., Yamauchi, Y., Chen, A.Z., Wu, K.C.W., 2020. Nanoarchitectured structure and surface biofunctionality of mesoporous silica nanoparticles. Adv. Mater. 32, 1–27. https://doi.org/10.1002/adma.201907035.
Karim, A.H., Jalil, A.A., Triwahyono, S., Sidik, S.M., Kamarudin, N.H.N., Jusoh, R., Jusoh, N.W.C., Hameed, B.H., 2012. Amino modified mesostructured silica nanoparticles for efficient adsorption of methylene blue. J. Colloid Interface Sci. https://doi.org/10.1016/j.jcis.2012.07.043.
Kimbell, L.K., Wang, Y., McNamara, P.J., 2020. The impact of metal pipe materials, corrosion products, and corrosion inhibitors on antibiotic resistance in drinking water distribution systems. Appl. Microbiol. Biotechnol. 104, 7673–7688. https://doi.org/10.1007/s00253-020-10777-8.
Kumar, K.V., Gadipelli, S., Wood, B., Ramisetty, K.A., Stewart, A.A., Howard, C.A., Brett, D.J.L., Rodriguez-Reinoso, F., 2019. Characterization of the adsorption site energies and heterogeneous surfaces of porous materials. J. Mater. Chem. 7, 10104–10137. https://doi.org/10.1039/c9ta00287a.
Kumar, S., Malik, M.M., Purohit, R., 2017. ScienceDirect synthesis methods of mesoporous silica materials. Mater. Process. 4, 350–357.
Largitte, L., Pasquier, R., 2016. A review of the kinetics adsorption models and their application to the adsorption of lead by an activated carbon. Chem. Eng. Res. Des. 109, 495–504. https://doi.org/10.1016/j.cherd.2016.02.006.
Lee, J.E., Mun, H., Kim, S.R., Kim, M.G., Chang, J.Y., Shim, W.B., 2020. A colorimetric Loop-mediated isothermal amplification (LAMP) assay based on HRP-mimicking molecular beacon for the rapid detection of Vibrio parahaemolyticus. Biosens. Bioelectron. 151 https://doi.org/10.1016/j.bios.2019.111968.
Leonel, A.G., Mansur, A.A.P., Mansur, H.S., 2021. Advanced Functional Nanostructures Based on Magnetic Iron Oxide Nanomaterials for Water Remediation: A Review. Water Res. https://doi.org/10.1016/j.watres.2020.116693.
Li, X., Zhang, J., Gu, H., 2012. Study on the adsorption mechanism of DNA with mesoporous silica nanoparticles in aqueous solution. Langmuir 28, 2827–2834. https://doi.org/10.1021/la204443j.
Maduraiveeran, G., Sasidharan, M., Jin, W., 2019. Earth-abundant transition metal and metal oxide nanomaterials: synthesis and electrochemical applications. Prog. Mater. Sci. https://doi.org/10.1016/j.pmatsci.2019.100574.
Miyah, Y., Lahrichi, A., Idrissi, M., Khalil, A., Zerrouq, F., 2018. Adsorption of methylene blue dye from aqueous solutions onto walnut shells powder: equilibrium and kinetic studies. Surface. Interfac. https://doi.org/10.1016/j.surfin.2018.03.006.
Osode, A.N., Okoh, A.I., 2009. Impact of discharged wastewater final effluent on the physicochemical qualities of a receiving watershed in a suburban community of the eastern Cape Province. Clean 37, 938–944. https://doi.org/10.1002/clen.200900098.
Panahi, A.H., Ashrafi, S.D., Kamani, H., Khodadadi, M., Lima, E.C., Mostafapour, F.K., Mahvi, A.H., 2019. Removal of cephalexin from artificial wastewater by mesoporous silica materials using box-behnken response surface methodology. Desalination Water Treat. 159, 169–180. https://doi.org/10.5004/dwt.2019.24109.
Panão, C.O., Campos, E.L.S., Lima, H.H.C., Rinaldi, A.W., Lima-Tenório, M.K., Tenório-Neto, E.T., Guilherme, M.R., Asefa, T., Rubira, A.F., 2019. Ultra-absorbent hybrid hydrogel based on alginate and SiO2 microspheres: a high-water-content system for removal of methylene blue. J. Mol. Liq. https://doi.org/10.1016/j.molliq.2018.11.157.
Qiao, B., Liang, Y., Wang, T.J., Jiang, Y., 2016. Surface modification to produce hydrophobic nano-silica particles using sodium dodecyl sulfate as a modifier. Appl. Surf. Sci. 364, 103–109. https://doi.org/10.1016/j.apsusc.2015.12.116.
Rodriguez-Mozaz, S., Chamorro, S., Marti, E., Huerta, B., Gros, M., Sànchez-Melsió, A., Borrego, C.M., Barceló, D., Balcázar, J.L., 2015. Occurrence of antibiotics and antibiotic resistance genes in hospital and urban wastewaters and their impact on the receiving river. Water Res. 69, 234–242. https://doi.org/10.1016/j.watres.2014.11.021.
Salehtash, F., Jalaly, M., Motejadded Emrooz, H.B., Gotor, F.J., Sayagués, M.J., 2018. Mesoporous silica by solution-combustion synthesis followed by etching. Int. J. Self-Propag. High-Temp. Synth. 27, 221–227. https://doi.org/10.3103/S1061386218040064.
Saman, N., Sakinah, N., Chew, L., Hamidah, S., Setapar, M., 2020. Cetyltrimethylammonium bromide functionalized silica nanoparticles (MSN) synthesis using a combined sol-gel and adsorption steps with enhanced adsorption performance of oxytetracycline in aqueous solution. J. Taiwan Inst. Chem. Eng. 1–11, 000.
Shao, S., Hu, Y., Cheng, J., Chen, Y., 2018. Research progress on distribution, migration, transformation of antibiotics and antibiotic resistance genes (ARGs) in aquatic environment. Crit. Rev. Biotechnol. 38, 1195–1208. https://doi.org/10.1080/07388551.2018.1471038.
Sharmiladevi, S., Shanmuga Priya, A., Sujitha, M.V., 2016. Synthesis of mesoporous silica nanoparticles and drug loading for gram positive and gram-negative bacteria. Int. J. Pharm. Pharmaceut. Sci. 8, 196–201.
Simonin, J.P., 2016. On the comparison of pseudo-first order and pseudo-second order rate laws in the modeling of adsorption kinetics. Chem. Eng. J. 300, 254–263. https://doi.org/10.1016/j.cej.2016.04.079.
Siqueira, T.C.A., da Silva, I.Z., Rubio, A.J., Bergamasco, R., Gasparotto, F., Paccola, E.A. de S., Yamaguchi, N.U., 2020. Sugarcane bagasse as an efficient biosorbent for methylene blue removal: kinetics, isotherms and thermodynamics. Int. J. Environ. Res. Publ. Health 17. https://doi.org/10.3390/ijerph17020526.
Soares, D.C.F., De Sousa Andrada, A., Ramaldes, G.A., 2015. Silica nanoparticles containing gadolinium complex as potential alternative to anticancer radiotherapy. Part. Sci. Technol. 33, 331–338. https://doi.org/10.1080/02726351.2014.970306.
Solberg, S.M., Landry, C.C., 2006. Adsorption of DNA into mesoporous silica. J. Phys. Chem. B 110, 15261–15268. https://doi.org/10.1021/jp061691+.
Spoial, A., Ficai, D., Ficai, D., Andronescu, E., 2020. Mesoporous silica platforms with potential applications in release and adsorption of active agents. Mol. MDPI 25, 2–35.
Titilawo, Y., Obi, L., Okoh, A., 2015. Occurrence of virulence gene signatures associated with diarrhoeagenic and non-diarrhoeagenic pathovars of Escherichia coli isolates from some selected rivers in South-Western Nigeria. BMC Microbiol. 15, 1–14. https://doi.org/10.1186/s12866-015-0540-3.
Uddin, M.T., Rahman, M.A., Rukanuzzaman, M., Islam, M.A., 2017. A potential low cost adsorbent for the removal of cationic dyes from aqueous solutions. Appl. Water Sci. 7, 2831–2842. https://doi.org/10.1007/s13201-017-0542-4.
Vandeventer, P.E., Lin, J.S., Zwang, T.J., Nadim, A., Johal, M.S., Niemz, A., 2012. Multiphasic DNA adsorption to silica surfaces under varying buffer, pH, and ionic strength conditions. J. Phys. Chem. B 116, 5661–5670. https://doi.org/10.1021/jp3017776.
Vazquez, N.I., Gonzalez, Z., Ferrari, B., Castro, Y., 2017. Synthesis of mesoporous silica nanoparticles by sol-gel as nanocontainer for future drug delivery applications. Bol. la Soc. Esp. Ceram. y Vidr. 56, 139–145. https://doi.org/10.1016/j.bsecv.2017.03.002.
Vilà, N., de Oliveira, P., Walcarius, A., Mbomekallé, I.M., 2019. pH-modulated ion transport and amplified redox response of Keggin-type polyoxometalates through vertically-oriented mesoporous silica nanochannels. Electrochim. Acta 309, 209–218. https://doi.org/10.1016/j.electacta.2019.03.119.
Wang, Y., Zhou, Y., Zhang, T., He, M., Bu, X., 2014. Two-dimensional ultrathin nanosheets of Ni-In-layered double hydroxides prepared in water: enhanced performance for DNA adsorption. RSC Adv. 4, 29968–29974. https://doi.org/10.1039/c3ra47728b.
Yang, S., Zhao, F., Sang, Q., Zhang, Y., Chang, L., Huang, D., Mu, B., 2021. Investigation of 3-aminopropyltriethoxysilane modifying attapulgite for Congo red removal: mechanisms and site energy distribution. Powder Technol. https://doi.org/10.1016/j.powtec.2021.01.046.
Yusuff, A.S., Popoola, L.T., Babatunde, E.O., 2019. Adsorption of cadmium ion from aqueous solutions by copper-based metal organic framework: equilibrium modeling and kinetic studies. Appl. Water Sci. 9 https://doi.org/10.1007/s13201-019-0991-z.
Zainab, S.M., Junaid, M., Xu, N., Malik, R.N., 2020. Antibiotics and Antibiotic Resistant Genes (ARGs) in Groundwater: A Global Review on Dissemination, Sources, Interactions, Environmental and Human Health Risks.
Zhang, X., Servos, M.R., Liu, J., 2012. Surface science of DNA adsorption onto citrate-capped gold nanoparticles. Langmuir 28, 3896–3902. https://doi.org/10.1021/la205036p.